



New lacunar-type and pendant groups containing derivatives of β -unsubstituted dibenzotetraaza[14]annulenes—syntheses and crystal structures

Jarosław Grolík^a, Paulina M. Dominiak^b, Lesław Sieroń^c, Krzysztof Woźniak^b, Julita Eilmes^{a,*}

^a Department of Chemistry, Jagiellonian University, Ingardena 3, 30-060 Kraków, Poland

^b Department of Chemistry, Warsaw University, Pasteura 1, 02-093 Warszawa, Poland

^c Institute of General and Ecological Chemistry, Technical University of Łódź, Żeromskiego 116, 90-924 Łódź, Poland

ARTICLE INFO

Article history:

Received 14 February 2008

Received in revised form 9 May 2008

Accepted 30 May 2008

Available online 5 June 2008

Keywords:

Dibenzotetraaza[14]annulene

Lacunar macrocycle

Crystal structure

C–H $\cdots\pi$

$\pi\cdots\pi$ Interactions

Self-assembly

ABSTRACT

Three new lacunar-type derivatives of β -unsubstituted dibenzotetraaza[14]annulene have been synthesized along with a range of their open-chain pendant group containing counterparts. The crystal structures of two representative products have been determined and the noncovalent interactions explored. A number of C–H $\cdots\pi$ and $\pi\cdots\pi$ interactions involving aliphatic chains and aromatic regions of the macrocycle have been evidenced. The relative ease and high yield of lacunization are suggested to be largely due to self-assembly processes, driven by favorable noncovalent interactions between reacting units.

© 2008 Elsevier Ltd. All rights reserved.

1. Introduction

Dibenzotetraaza[14]annulenes (Fig. 1) belong to the class of tetraaza macrocycles of bioinorganic relevance, known and appreciated for their synthetic accessibility and rich chemistry.¹ So far, research interest in this area has been focused mainly on β -substituted macrocycles ($R \neq H$). Important features in which β -substituted dibenzotetraaza[14]annulenes differ from the unsubstituted analogs ($R=H$) lie in their three-dimensional molecular structure. As shown by crystallography, the molecules are flat when $R=H$.² In contrast, they adopt a saddle-like conformation

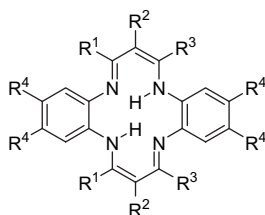


Figure 1.

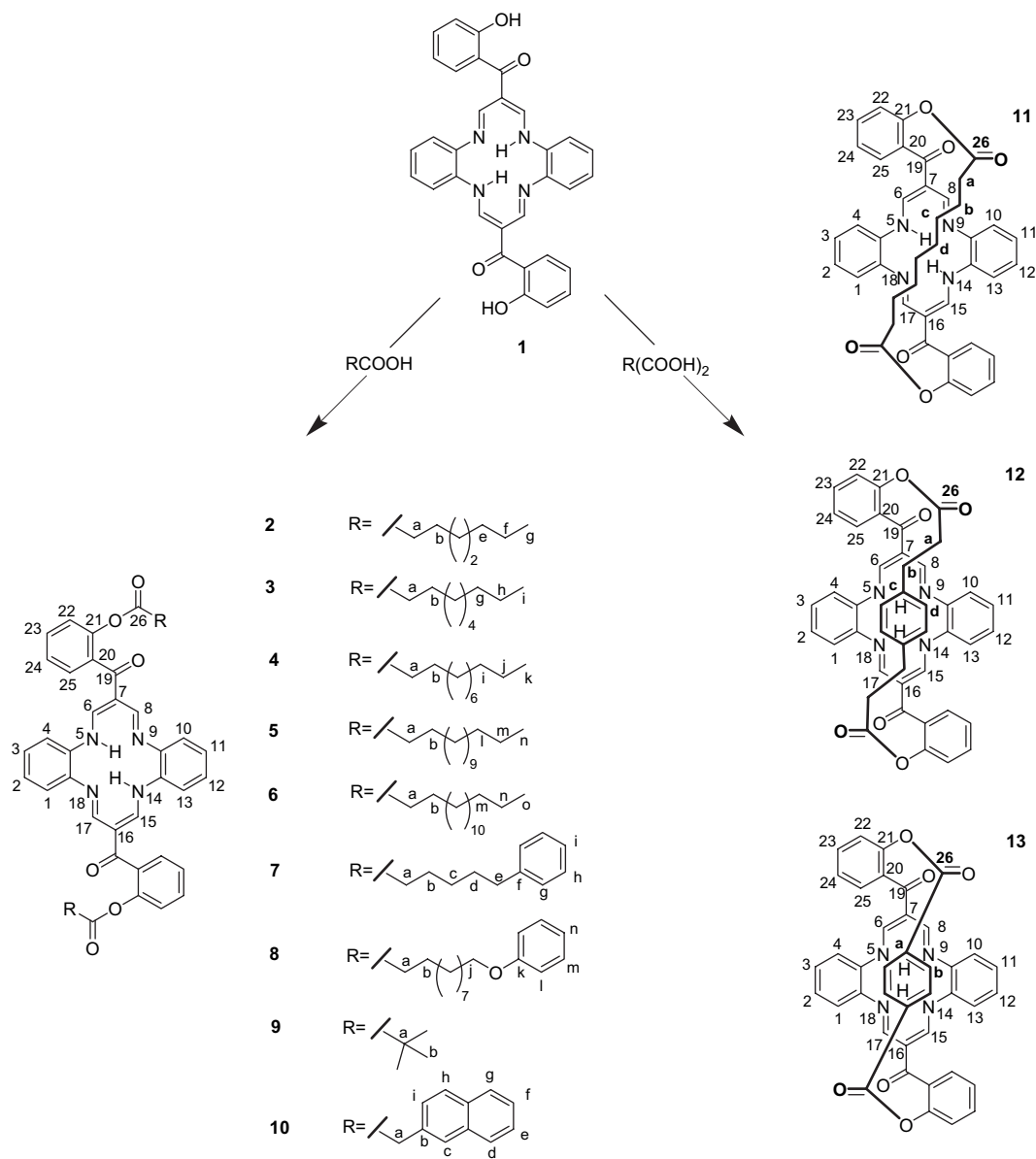
when $R \neq H$ because of the steric hindrance between substituents R and the phenylene protons.^{3a,b} It is worth mentioning here that analogous distortion of planarity induced by similarly positioned alkyl group was observed by Desiraju et al. in the crystal structure of 11-ethyl-15,16-dihydrocyclopenta[a]phenantren-17-one.^{3c,d}

The conformation of the macrocyclic ring greatly influences the reactivity and coordination properties of dibenzotetraaza[14]annulene ligands. Nonplanar dibenzotetraaza[14]annulene ligands were found to be highly reactive and offered a variety of coordination modes and geometries, thus giving rise to a vast number of main group and transition metal complexes.^{3b} Also in the area of supramolecular chemistry, the noncovalent interactions appeared to rely mainly on complementarity between curved concave surfaces of saddle-shaped molecules and corresponding convex shapes of various globular guests.⁴ Similarly, clathrate formation involving solvent molecules arises from the inefficiencies of the packing of nonplanar, saddle-like molecules.⁵

In contrast to the wealth of coordination chemistry and to remarkable synthetic achievements reported for saddle-shaped dibenzotetraaza[14]annulenes (where R_1, R_3 is a methyl group), their planar analogs seem to be relatively under investigated. We have recently found that the dicationic, water-soluble derivatives of β -unsubstituted macrocycle exhibited DNA/RNA binding properties.⁶ It also appeared that the introduction of four 3,7-dimethyloctyloxy substituents to the phenylene part of the macrocyclic core allowed for the generation of a liquid-crystalline behavior.^{2d}

* Corresponding author. Tel.: +48 12 6632294; fax: +48 12 6340515.

E-mail address: jeilmes@chemia.uj.edu.pl (J. Eilmes).



Scheme 1.

In this paper, we report on the preparation of new pendant groups containing **2–10** and lacunar derivatives (**11–13**) of planar β -unsubstituted dibenzotetraaza[14]annulene. As before, here again we used γ,γ -bis(2-hydroxybenzoyl) derivative **1** as a substrate well suited for synthetic modification, due to its reactive OH groups. The reactivity of these groups and their alignments within the molecule^{2d} also seemed to be useful for the preparation of bridged derivatives, often referred to as lacunar-type macrocycles. The synthetic route to these new products is shown in Scheme 1.

2. Results and discussion

2.1. Synthesis

New products **2–10** bearing open-chain pendant substituents have been prepared via ester-linkages-creating couplings of **1** with appropriate carboxylic acids. Coupling procedures using *N,N*-diisopropylcarbodiimide (DIC) as a dehydrating agent⁷ and 4-dimethylaminopyridine (DMAP) as an acylation catalyst⁸ have been successfully employed affording products **2–10** with yields

increasing remarkably with the length of the polymethylene chains, ranging from 19% to 86%.

A similar esterification of **1**, with the use of dicarboxylic acids, gave rise to macrobicyclic lacunar-type derivatives **11–13**. Surprisingly, the yields of the lacunar products appeared relatively high (41–64%) without recourse to the high dilution technique usually employed for the bridging of planar macrocycles such as porphyrins⁹ or Schiff-base complexes.¹⁰ This also contrasted positively with the data reported by Raston, who, using a high dilution procedure, had recently afforded γ,γ -strapped dibenzotetraaza[14]annulenes in only 26% and 39% yields.¹¹ Our results seemed even more unexpected considering that Raston was working with saddle-shaped macrocycles, which are known for their higher propensity to be bridged.¹² As shown by Busch in his work on macrocyclic *cyclidenes*, saddle-like conformation of the precursor molecules facilitates lacunization by directing the reactive functional groups to the same side of the N4 plane.^{12a,b}

In order to get more insight into the lacunization of the planar dibenzotetraaza[14]annulenes, we have focused our attention on three-dimensional structures and on noncovalent interactions

within the molecules of the new derivatives. As the molecules contained C=O and OH groups, benzene rings, and aromatic pentanediiiminate moieties, therefore, they seemed suitable for careful searching of C–H \cdots O,^{3c} C–H \cdots π ,^{13a–c} and $\pi\cdots\pi$ ¹⁴ motifs and accounting for their role in the crystal engineering and the supramolecular synthesis.

2.2. Crystallography

Here, we report the crystal structures of product **2** and of three crystalline modifications of the lacunar product **11** (**a–c**). Crystal data and other parameters related to data collection for all structures are summarized in Table 1. All molecular structures of the products **2** and **11** are shown in Figure 2.

2.2.1. Compound 2

Compound **2** crystallizes in the monoclinic $P2_1/c$ space group and the asymmetric unit consists of two half molecules. The center of the molecule lies at the crystallographic center of symmetry. The molecule of **2** has two open aliphatic chains folded above the tetraaza ring with approximate distance of 4 Å. Its overall conformation is defined by five torsion angles with descriptors of ap/ap/sc/sc/ap corresponding to the atom order from C(17) to C(24). This spatial orientation of the aliphatic chain comes probably from its attractive intramolecular C–H \cdots π contacts with N–C bonds of the tetraaza macrocyclic ring (there are six contacts of the type C–H \cdots [N–C]_{mid-point}, ranging from 2.85 to 3.06 Å), similar to molecule **1**. On the other hand, the effect of the repulsive interaction between the hydrophobic methylene groups of adjacent aliphatic chains is also observed, as shown in Figure 3. The shortest intermolecular non-bonded H \cdots H separation between aliphatic chains is 2.55(3) Å.

The oxygen atom of the keto group is involved in bifurcated O \cdots H–C intermolecular contacts with phenyl rings (Table 2). The dihedral angle between planes of benzoyl and tetraaza rings is 59.46(3)°. The carbonyl O(3) atom is engaged in three weak C–H \cdots O interactions to two neighboring molecules. There is no evidence of significant $\pi\cdots\pi$ contacts between benzene rings in the structure of **2**.

2.2.2. Lacunar product 11

Compound **11** crystallizes in different space groups and crystal systems depending on the solvent molecules incorporated into crystal lattice. In the case of chloroform (**11a**), it crystallizes in the orthorhombic $Pbcn$ space group with one half of the tetraaza fragment and almost one half of chloroform molecule in the asymmetric part of the unit cell (Fig. 4). In fact, the solvent molecule is disordered over two positions and required some geometrical restraint during refinement. Slow diffusion of water into the solution of **11** in *N,N*-dimethylformamide (DMF) gave **11b** crystals in triclinic $P-1$ space group with one tetraaza and ca. 20% of water molecule in the asymmetric part of the unit cell (**11b**, Fig. 5). The solvent molecule is placed in a special position and was refined only with an isotropic model of displacement parameter. A crystallization of **11** from DMF/diisopropyl ether gave non-solvated **11c** crystals in monoclinic $P2_1/n$ space group with two independent molecules in the asymmetric unit (Fig. 7).

2.2.2.1. Crystals of the chloroform solvate 11a. In the crystals of the chloroform solvate (**11a**), the molecules of **11** form channels along the *c* axis inside which solvent molecules are located. The channels have roughly rectangular cross-sections (9.3 \times 6.4 Å²) with the longer side built by the tetraaza macrocyclic fragments and the shorter one by the benzoyl rings of the macrocycle molecules. The molecules from one channel are in contact with the molecules from another either through benzoyl rings or aliphatic chains (see Figs. 4b and 6a). However, the disordered chloroform molecule tends to orient its hydrogen atom toward the tetraaza plane of the nearest molecule of **11** and two out of three chlorine atoms toward the benzoyl substituents of the molecules from the opposite side of the channel.

To form a channel, the molecules of **11** adopt saddle-like conformation with propylenediimine fragments on the side of the tetraaza plane opened to the solvent molecules and the phenylene rings on the side where the aliphatic chain is located. The curvature of the macrocycle is of reasonable magnitude as indicated by the angle between the mean planes of the propylenediimine fragments equal to 35.9° and the angle between the mean planes of phenylene rings, which is 31.8°. The benzoyl substituents are oriented nearly

Table 1
Crystal data and structural refinement details for **2** and **11a–c**

	2	11a	11b	11c
Empirical formula	C ₄₈ H ₅₂ N ₄ O ₆	C ₄₂ H ₃₈ N ₄ O ₆ ·0.80CHCl ₃	C ₄₂ H ₃₈ N ₄ O ₆ ·0.20H ₂ O	C ₄₂ H ₃₈ N ₄ O ₆
Formula weight	780.94	790.26	698.36	694.76
Crystal system	Monoclinic	Orthorhombic	Triclinic	Triclinic
Space group	$P2_1/c$	$Pbcn$	$P-1$	$P2_1/n$
<i>a</i> (Å)	8.3215(3)	22.211(2)	11.337(3)	22.775(2)
<i>b</i> (Å)	11.1341(3)	14.2721(13)	11.622(4)	11.3284(10)
<i>c</i> (Å)	21.8296(6)	12.4810(12)	13.921(5)	27.117(2)
α (°)	90	90	89.33(3)	90
β (°)	96.287(2)	90	75.65(3)	97.184(1)
γ (°)	90	90	77.15(3)	90
<i>V</i> (Å ³), <i>Z</i>	2010.40(11), 2	3956.4(6)	1730.7(10), 2	6941.4(10), 8
<i>d</i> _{calc} (g/cm ³)	1.290	1.329	1.339	1.330
<i>F</i> (000)	832	1656	735	2928
Temperature (K)	100	85	200	90
Radiation type, wavelength (Å)	Mo K α , 0.71073	Mo K α , 0.71073	Mo K α , 0.71073	Mo K α , 0.71073
μ (mm ^{−1})	0.085	0.218	0.091	0.090
θ Range (°)	1.88–27.00	2.35–25.00	2.97–25.00	1.51–25.00
Limiting indices, <i>h</i> , <i>k</i> , <i>l</i>	−9 \rightarrow 10, −14 \rightarrow 14, −27 \rightarrow 25	−26 \rightarrow 26, −16 \rightarrow 16, −14 \rightarrow 14	−13 \rightarrow 13, −13 \rightarrow 13, −16 \rightarrow 16	−27 \rightarrow 27, −13 \rightarrow 13, −32 \rightarrow 32
Reflections collected	16,559	45,010	25,433	98,380
Unique reflections	4369 [<i>R</i> _{int} =0.026]	3482 [<i>R</i> _{int} =0.026]	6086 [<i>R</i> _{int} =0.102]	12,232 [<i>R</i> _{int} =0.030]
Completeness to $\theta=25.00^\circ$	99.9%	99.8%	99.8%	100.0%
Data/restraints/parameters	4369/0/366	3482/4/340	6086/0/471	12,232/0/1025
Goodness-of-fit on <i>F</i> ²	1.079	1.053	0.796	1.054
Final <i>R</i> indices [<i>I</i> >2 σ (<i>I</i>)]	<i>R</i> =0.0374, <i>wR</i> ² =0.0981	<i>R</i> =0.0511, <i>wR</i> ² =0.1393	<i>R</i> =0.0489, <i>wR</i> ² =0.0897	<i>R</i> =0.0317, <i>wR</i> ² =0.0826
Final <i>R</i> indices [all data]	<i>R</i> =0.0522, <i>wR</i> ² =0.1045	<i>R</i> =0.0543, <i>wR</i> ² =0.1418	<i>R</i> =0.1430, <i>wR</i> ² =0.1163	<i>R</i> =0.0384, <i>wR</i> ² =0.0861
Largest diff. peak and hole (e Å ^{−3})	0.266, −0.185	0.943, −0.566	0.277, −0.287	0.249, −0.216

Compound **2**: weight= $1/[\sigma^2(F_0^2)+(0.0535P)^2+0.3805P]$ where $P=(\max(F_0^2,0)+2F_c^2)/3$, compound **11a**: weight= $1/[\sigma^2(F_0^2)+(0.0730P)^2+4.6542P]$ where $P=(\max(F_0^2,0)+2F_c^2)/3$, compound **11b**: weight= $1/[\sigma^2(F_0^2)+(0.0345P)^2]$ where $P=(\max(F_0^2,0)+2F_c^2)/3$, and compound **11c**: weight= $1/[\sigma^2(F_0^2)+(0.0436P)^2+2.1418P]$ where $P=(\max(F_0^2,0)+2F_c^2)/3$.

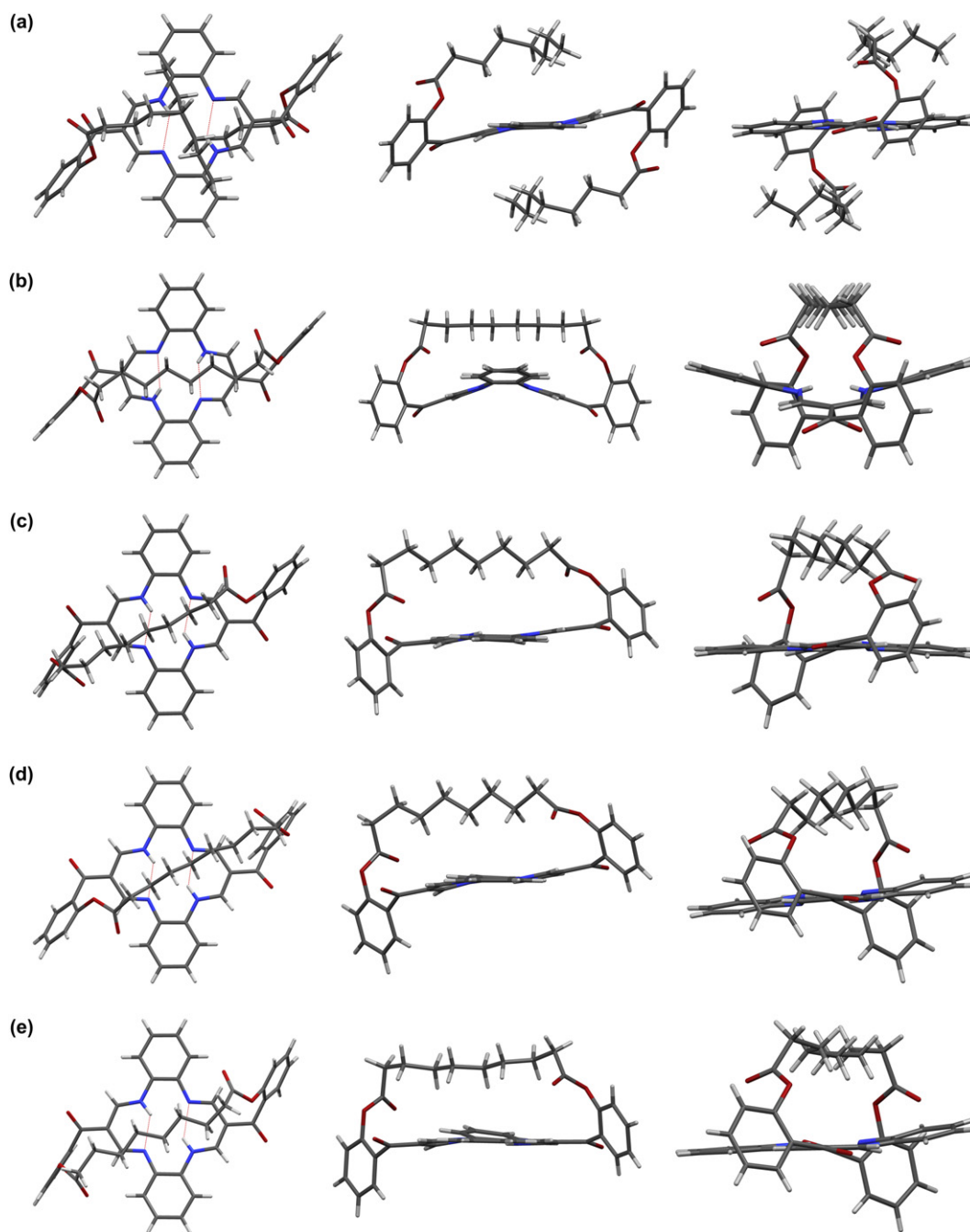


Figure 2. Three perpendicular views of the molecules of the products **2** and **11**: (a) **2**, (b) **11a**, (c) **11b**, (d) **11c** (molecule I), and (e) **11c** (molecule II).

perpendicular to the tetraaza plane with angle of $88.9(2)^\circ$ and contribute to the formation of the solvent channel.

The aliphatic chain in **11a** adopts a nearly planar extended conformation. The plane formed by aliphatic carbons is parallel to the tetraaza fragment and only 3.47 \AA distant from it. Consequently, the $\text{H}(20\text{A})^{-x+1,y,-z+3/2}$ and $\text{H}(21\text{A})$ atoms form short contacts with the $\text{N}(2)-\text{C}(7)$ and $\text{N}(1)-\text{C}(2)$ bonds, respectively. These may be classified as moderately strong $\text{Csp}^3-\text{H}\cdots\pi$ interactions since the $\text{H}\cdots$ midpoint distances of $2.72(8)$ and $2.62(8) \text{ \AA}$, respectively, are well below the 3.14 \AA limit, which is considered still as an attractive interaction.¹⁵

As for intermolecular interactions, the molecules of the macrocycle have oxygen atoms with a possibility to accept a hydrogen atom to form hydrogen bonding. Since the only hydrogen donors accessible for intermolecular interactions are carbon atoms, weak $\text{C}-\text{H}\cdots\text{O}$ hydrogen bonds are utilized to assemble the molecules.

Two of these H-bonds, $\text{C}(13)-\text{H}(13)\cdots\text{O}(1)$ (Table 2), formed between the keto groups from one and benzoyl ring from another molecule of **11** are the only direct interactions between molecules forming the solvent channel. Similarly, the $\text{C}(21)-\text{H}(21\text{B})\cdots\text{O}(3)^{x,-y+1,z+1/2}$ weak hydrogen bonds (Table 3) are the only contacts below the van der Waals sum observed for two channels oriented to each other with their aliphatic chains. However, the aliphatic chains interlace with each other to build a zip-lock-like structure maximizing packing efficiency.^{16a,b}

Numerous interactions are observed for channels oriented to each other with their benzoyl rings. These are either $\text{C}-\text{H}\cdots\text{O}$ hydrogen bonds $[\text{C}(4)-\text{H}(4)\cdots\text{O}(1)^{3/2-x,1/2-y,1/2+z}]$ and $[\text{C}(15)-\text{H}(15)\cdots\text{O}(1)^{3/2-x,1/2-y,-1/2+z}]$ or $\text{C}-\text{H}\cdots\pi$ interaction $[\text{C}(3)-\text{H}(3)\cdots\text{C}_g(1)^{3/2-x,1/2-y,1/2+z}]$ (Table 3). The latter can be classified as of type II, according to Malone et al.^{13a}

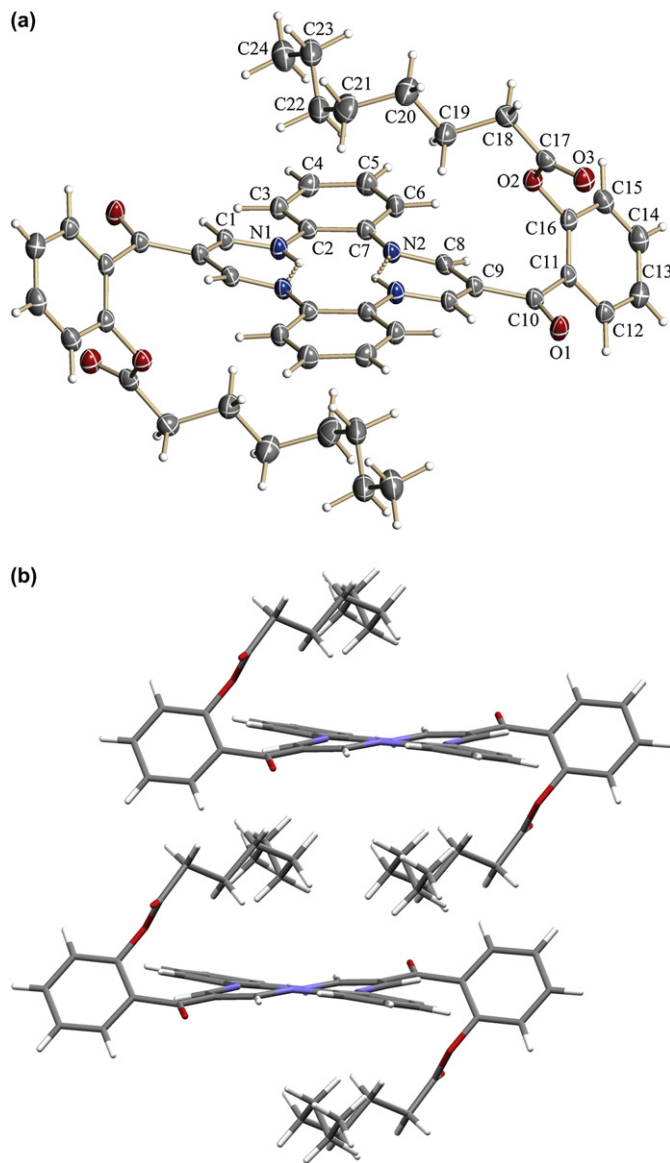


Figure 3. (a) An ORTEP view of **2** with numbering scheme. Displacement ellipsoids are drawn at the 50% probability level. Unlabeled atoms are related to labeled atoms by the symmetry code $-x+1, -y+1, -z+1$. Hydrogen atoms are drawn with an arbitrary radius. (b) A view of reciprocal interaction between hydrophobic aliphatic chains of neighboring molecules of **2**.

2.2.2.2. Crystals of the hydrate 11b. In the crystals of the hydrate (**11b**), the molecule of **11** seems to be more relaxed. The macrocyclic part is planar as is usual for such modestly substituted dibenzotetraaza[14]annulenes.² The benzoyl rings are oriented in respect to the tetraaza plane in a similar way as in **11a**. However, the angles between the rings and the plane are smaller [81.89(8) and 71.89(7)° for rings C(11–16) and C(27–32), respectively].

There are no solvent channels in the **11b** structure. Planar tetraazamacrocycles are now much closer to each other as indicated by the 3.44 Å distance between mean tetraaza planes (was 6.04 Å for **11a**). Molecules are still shifted in respect to each other (by 4.45 Å) to maximize the $\pi \cdots \pi$ interactions between the tetraaza macrocyclic rings. Such dimers form a strand in the direction topologically perpendicular to the direction of a channel in **11a** structure (Figs. 5b and 6b).

As for the aliphatic chain, it is still in an extended conformation but its length is 0.064 Å shorter than that in the chloroform solvate structure (**11a**). The aliphatic carbon atom plane is no longer

Table 2
Close contacts of hydrogen bond type [Å and °]

D–H...A	H...A	D...A	D–H...A
2			
C(1)–H(1)...O(3) ^{x,3/2–y,1/2+z}	2.48	3.5195(15)	161
C(3)–H(3)...O(3) ^{x,3/2–y,1/2+z}	2.43	3.3113(16)	138
C(4)–H(4)...O(1) ^{x,3/2–y,1/2+z}	2.61	3.5370(16)	143
C(15)–H(15)...O(1) ^{1–x,1/2+y,1/2–z}	2.62	3.3236(18)	122
C(15)–H(15)...O(3) ^{1–x,1/2+y,1/2–z}	2.46	3.3067(16)	134
C(3)–H(3)...C _g (1) ^{x,3/2–y,1/2+z}	2.88	3.7338(14)	136
C _g (1)=centroid C(11–16)			
11a			
C(13)–H(13)...O(1) ^{x,–y,–1/2+z}	2.24	3.311(9)	170
C(15)–H(15)...O(1) ^{3/2–x,1/2–y,–1/2+z}	2.28	3.215(8)	144
C(21)–H(21B)...O(3) ^{x,–y+1,1/2}	2.54	3.608(8)	169
C(4)–H(4)...O(1) ^{3/2–x,1/2–y,1/2+z}	2.54	3.589(8)	164
C(3)–H(3)...C _g (1) ^{3/2–x,1/2–y,1/2+z}	2.82	3.850(7)	159
C _g (1)=centroid C(11–16)			
11b			
C(1)–H(1)...O(1) ^{–1+x,y,z}	2.49	3.574(4)	177
C(3)–H(3)...O(1) ^{–1+x,y,z}	2.26	3.319(4)	164
C(40)–H(40)...O(6) ^{–1+x,y,z}	2.26	3.331(4)	171
C(42)–H(42)...O(6) ^{–1+x,y,z}	2.43	3.514(4)	179
C(31)–H(31)...O(6) ^{2–x,2–y,–z}	2.43	3.448(4)	156
C(39)–H(39)...C(30) ^{–1+x,y,z}	2.72	3.786(4)	168
C(39)–H(39)...C(31) ^{–1+x,y,z}	2.75	3.637(4)	139
C(25)–H(25B)...O(3) ^{1–x,2–y,1–z}	2.57	3.631(4)	165
C(19)–H(19B)...O(5) ^{1–x,2–y,1–z}	2.60	3.567(4)	148
C(23)–H(23A)...C(4) ^{1–x,2–y,1–z}	2.92	3.816(4)	140
C(23)–H(23A)...C(5) ^{1–x,2–y,1–z}	2.94	3.724(4)	129
C(5)–H(5)...O(3) ^{1–x,1–y,1–z}	2.28	3.321(4)	160
C(13)–H(13)...C _g (1) ^{x,–1+y,z}	2.62	3.682(4)	165
C _g (1)=centroid C(36–41)			
11c			
C(6)–H(6)...O(6) ^{x,1+y,z}	2.22	3.2945(14)	172
C(8)–H(8)...O(6) ^{x,1+y,z}	2.39	3.4711(14)	175
C(15)–H(15)...O(14) ^{x,1+y,1+z}	2.51	3.4239(17)	141
C(18)–H(18A)...O(14) ^{1–x,1–y,1–z}	2.48	3.3647(17)	138
C(31)–H(31)...O(6) ^{3/2–x,y,3/2–z}	2.46	3.4967(16)	160
C(35)–H(35)...O(1) ^{x,–1+y,z}	2.46	3.5370(14)	175
C(37)–H(37)...O(1) ^{x,–1+y,z}	2.24	3.2925(15)	164
C(56)–H(56)...O(16) ^{x,1+y,z}	2.19	3.2654(14)	175
C(58)–H(58)...O(16) ^{x,1+y,z}	2.42	3.4983(14)	175
C(68)–H(68A)...O(4) ^{1–x,1–y,1–z}	2.41	3.3410(17)	144
C(78)–H(78)...O(3) ^{x,–1+y,–1+z}	2.31	3.2626(16)	145
C(81)–H(81)...O(16) ^{3/2–x,y,1/2–z}	2.26	3.3074(14)	163
C(85)–H(85)...O(11) ^{x,–1+y,z}	2.44	3.5153(14)	174
C(87)–H(87)...O(11) ^{x,–1+y,z}	2.23	3.3090(15)	176
C(89)–H(89)...O(13) ^{x,–1+y,z}	2.44	3.3255(16)	138
C(90)–H(90)...O(13)	2.34	3.3843(15)	162
C(13)–H(13)...C _g (1) ^{3/2–x,1+y,3/2–z}	2.47	3.4945(15)	157
C(63)–H(63)...C _g (2) ^{3/2–x,y,3/2–z}	2.51	3.5641(15)	164
C(69)–H(69A)...C _g (3) ^{1–x,1–y,1–z}	2.58	3.5083(15)	143
C _g (1)=centroid C(86–91); C _g (2)=centroid C(36–41); C _g (3)=centroid C(2–7)			

All C–H distances have been set at the neutron diffraction value of 1.08 Å.

parallel to the tetraaza one and the dihedral angle between them is 71.89(7)°. The aliphatic chain is also further away from the tetraaza plane, no contacts below the van der Waals sum are observed.

The carbonyl oxygens from the keto groups are involved in strengthening the interactions within one strand. The O(1) oxygen forms bifurcated hydrogen bonding with H(1) and H(3) of the tetraazamacrocyclic ring from neighboring coplanar molecule (Table 2). The O(6) oxygen maintains trifurcated hydrogen bonding with the H(40) and H(42) hydrogens of the tetraazamacrocyclic ring atoms from the coplanar neighboring molecule and one with the H(31) of the benzoyl ring from another non-coplanar molecule. The formation of the strand is additionally supported by C–H... π interactions. The aromatic H(39) atom of phenylene fragment interacts with the benzoyl ring of the coplanar molecule, mainly through the C(30) and C(31) atoms. This is type V of the C–H... π_{phenyl} interactions in the classifications of Malone et al.^{13a}

The strands in **11b** interact with each other in a way resembling the interactions of channels in **11a**. Here, there are also two modes

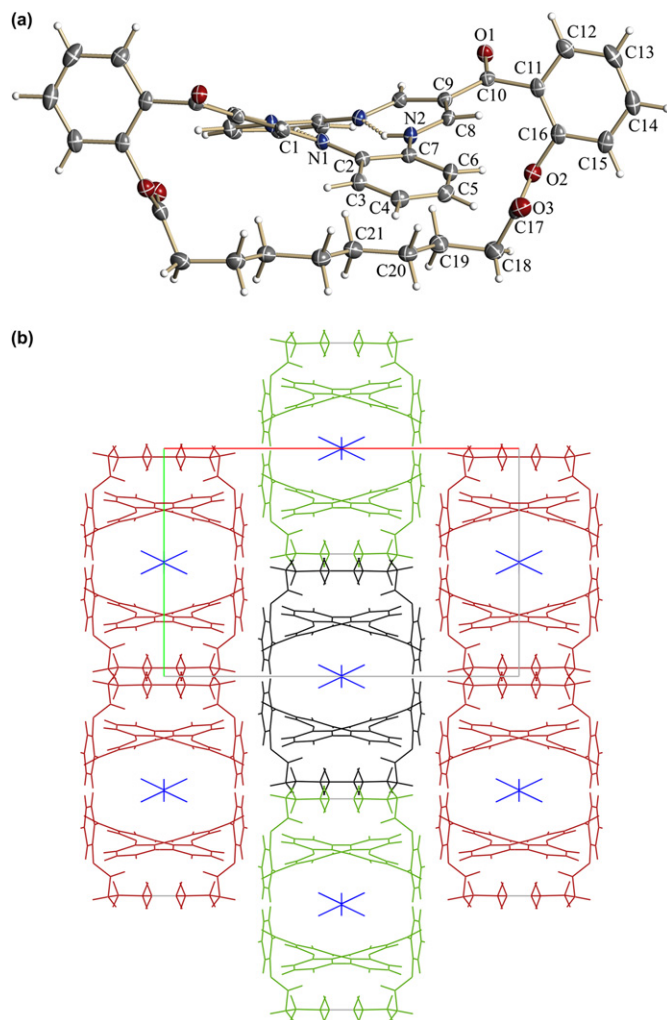


Figure 4. (a) An ORTEP view of main molecule of **11a** with numbering scheme. Displacement ellipsoids are drawn at the 50% probability level. Unlabeled atoms are related to labeled atoms by the symmetry code $-x+1, y, -z+3/2$. Hydrogen atoms are drawn with an arbitrary radius. The chloroform molecule has been omitted. (b) The crystal packing of **11a**. Molecules form a channel (perpendicular to the view, black) and interact with molecules from neighboring channels via either aliphatic chains (green) or benzoyl rings (dark red); view along the *c* axis.

of mutual contacts between aliphatic chain or benzoyl ring sides of molecules, see Figures 5b and 6b. Similarly, the aliphatic chains form a zipper-like structure but with larger number of contacts below the van der Waals sum. Four C–H \cdots O hydrogen bonds are observed: C(25)–H(25B) \cdots O(3) $^{1-x,2-y,1-z}$ and C(19)–H(19B) \cdots O(5) $^{1-x,2-y,1-z}$ and their symmetry related counterparts (Table 2), one C–H \cdots π_{phenyl} contact of type III [engaging H(23A), C(4), and C(5) atoms], and some H \cdots H van der Waals contacts. The interactions between strands maintained by benzoyl sides of molecules also include C–H \cdots O hydrogen bonding [C(5)–H(5) \cdots O(3) $^{1-x,1-y,1-z}$], C–H \cdots π_{phenyl} contact of type II [C(13)–H(13) \cdots C₆(2) $^{x,-1+y,z}$], and some H \cdots H contacts. In addition, the interactions of the O(4) oxygen are mediated by a disordered water molecule [O(4) \cdots O(1S) $^{x,1+y,z}=3.029(3)$ Å], which links the carbonyl oxygen with its symmetry related counterpart from the neighboring strand.

2.2.2.3. Crystals of the non-solvate 11c. In the crystals of the non-solvate **11c**, the asymmetric unit is composed of two independent molecules of **11** (Fig. 7). The molecules differ mainly in the orientation of their aliphatic chains in respect to the tetraaza plane, however, both adopt nearly planar extended conformation. A calculated dihedral angle defined between the mean planes of

aliphatic chain and 14-membered macrocyclic tetraaza ring is 74.90(10) and 7.62(6) $^\circ$ for molecule I and II, respectively.

The angles between the benzoyl rings and the tetraaza plane in molecule I are smaller than that in **11b** [77.64(3) and 69.01(3) $^\circ$ for rings C(11–16) and C(27–32), respectively] since in molecule II they are more similar [87.75(3) and 72.86(3) $^\circ$ for rings C(61–66) and C(77–82), respectively].

The supramolecular structure of compound **11c** is defined by extensive network of C–H \cdots O and C–H \cdots π interactions between molecules, as shown in Table 2.

Opposite to the crystals **11a** and **11b**, containing solvent molecules, the molecular packing of **11c** does not show neither channels nor strand arrangements in the structure. The reciprocal interactions between aliphatic chains of neighboring molecules can be observed, as shown in Figure 8.

2.2.2.4. Conformation of dibenzotetraazaannulene rings. In lacunar molecules (**11a–c**), the aliphatic chains adopt a nearly planar extended conformation. A comparison of dihedral angles between mean planes formed by aliphatic chains and tetraaza rings, and the deformation parameters of the tetraaza fragment are summarized in Table 3. A deformation from planarity was defined by interplanar angles between *o*-phenylene rings as well as by the mean plane of propanediminate fragments.

A planar conformation of the tetraaza ring is observed for nearly perpendicular location of the aliphatic chain plane (**11b** and **11c(I)**). When the aliphatic chain runs strictly parallel with the tetraaza ring mean plane, the conformation becomes significantly basket-like shaped (**11a**). A small deviation from this parallelism [7.62(6) $^\circ$] causes a slight flatness violation of the macrocyclic ring (**11c(II)**). A bending is, although not so distinct, also visible on the N–C–C–N based parameter. The closest distance of aliphatic chain H-atoms to the tetraaza ring mean plane is similar in all molecules and ranges from 2.62 to 2.75 Å, indicating the presence of some intramolecular chain–ring interactions.

2.2.2.5. *N4* planes—geometry of the hydrogen bonds. The positions of the hydrogen atoms connected to the nitrogen atoms and participating in the hydrogen bonds were located from the experimental difference electron density maps (except **11b** where all hydrogen atoms were fixed geometrically). Details of hydrogen bonds present in the structures are given in Table 4. The hydrogen bonds are relatively long [range of 2.04–2.10 Å] with small D–H \cdots A angles [range of 132–138 $^\circ$].

3. Conclusion

Three new lacunar-type derivatives of β -unsubstituted dibenzotetraaza[14]annulene have been synthesized for the first time and a range of their open-chain pendant group containing counterparts. The lacunar products have been prepared in respectable yields, without recourse to high dilution technique, via ester-linkages-creating condensations involving OH groups of **1** and COOH groups of appropriate carboxylic acids.

The crystallographic study revealed a number of noncovalent interactions, including C–H \cdots π , $\pi\cdots\pi$, and hydrogen bonds in the molecules of **2** and **11**. It appeared that OH groups of **1** were properly oriented in space and well suited so as to match the appropriate alignment of polymethylene chains with respect to the plane of the macrocycle and the distance allowing for favorable C–H \cdots π interactions. Thus, the molecule of **2** adopts a conformation with the aliphatic chains lying above and below the macrocyclic ring to maximize the number of C–H \cdots π contacts.

It seems reasonable to suppose that similar self-assembling interactions involving polymethylene chains and aromatic regions of the macrocycle may be responsible for the relative ease and high

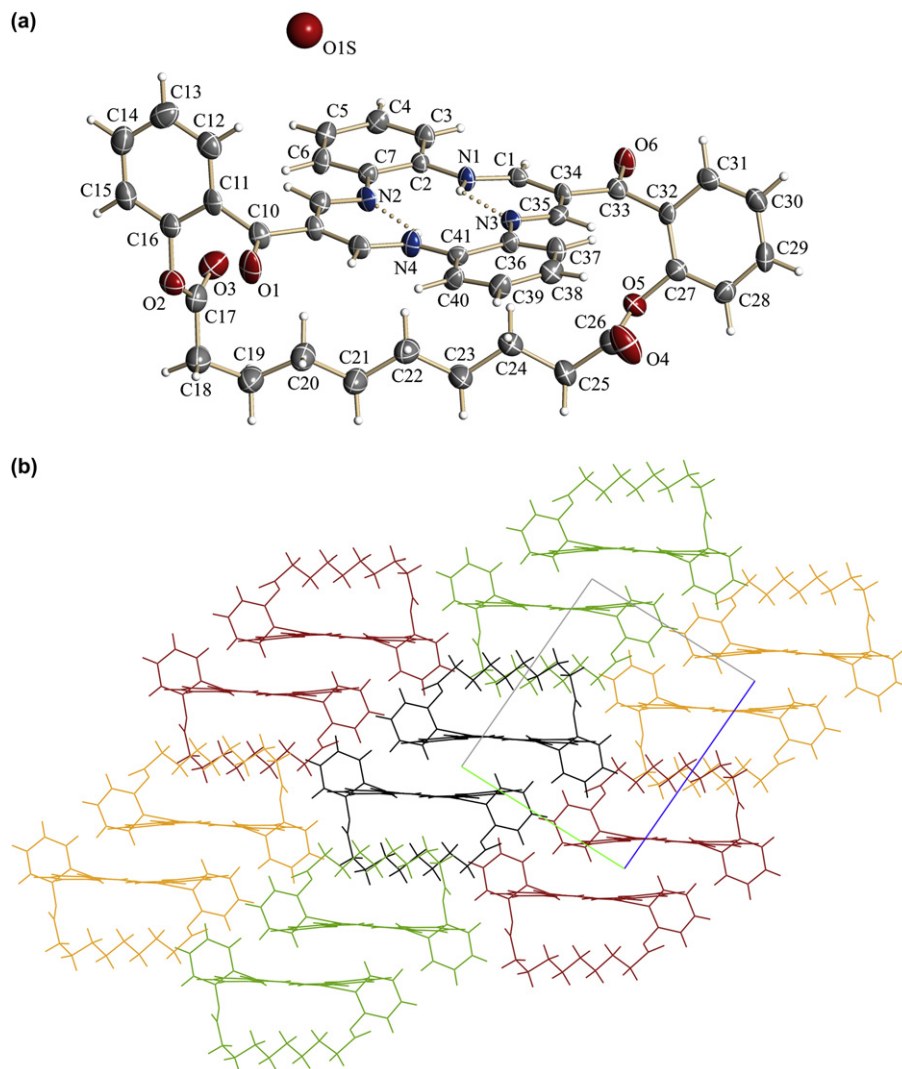


Figure 5. (a) An ORTEP view of main molecule of **11b** with numbering scheme. Displacement ellipsoids are drawn at the 50% probability level. Hydrogen atoms in disordered species are omitted and the other ones are drawn with an arbitrary radius. (b) The crystal packing of **11b**. Molecules of **11** form a strand (perpendicular to the view, black) and interact with molecules from neighboring strands via either aliphatic chains (green) or benzoyl rings (dark red, light red); view along the *a* axis.

yield of lacunization of **1** by means of dicarboxylic acids, leading to **11–13**. Assuming that there are no steric constraints in the free rotation of the *o*-hydroxybenzoyl groups of **1** around the C–C bonds, one can expect that such favorable noncovalent interactions involving substrate molecules may bring reactive OH and COOH groups into close proximity, thus facilitating a 1:1 condensation mode, yielding lacunar products. Alternatively, one can say that such self-assembling processes involving substrates may significantly suppress the tendency toward linear ‘head to tail’ couplings, which lead to oligomers and polymers. The incorporation of aromatic rings into the bridging precursor of **12** and **13** may even strengthen the self-assembling forces via additional $\pi \cdots \pi$ interactions.

As a conclusion for the synthetic chemists, the results described here suggest that careful design and incorporation of noncovalent interactions into molecular building blocks may be a successful strategy in the synthesis of more complex architectures.

4. Experimental

4.1. General

Macrocyclic substrate 7,16-bis(2-hydroxybenzoyl)-5,14-dihydrodibenzo[*b,i*][1,4,8,11]tetraazacyclotetradecine (**1**) was prepared by

the procedures described earlier.¹⁷ Other chemicals (*N,N*-diisopropylcarbodiimide (DIC), 4-dimethylaminopyridine (DMAP), and carboxylic acids) were purchased from commercial sources (Sigma–Aldrich, Fluka) and were used as-received. Solvents were dried using standard methods and were freshly distilled before use. Elemental analyses were performed on a Euro-EA (EuroVector) microanalyzer. ¹H and ¹³C NMR were run on a Bruker AMX (500 MHz) spectrometer. Chemical shifts (δ) are expressed in parts per million and *J* values in hertz. Signal multiplicities are denoted as s (singlet), d (doublet), t (triplet), q (quartet), and m (multiplet). ESI and MALDI-TOF mass spectra were taken on Esquire 3000 and Bruker Reflex IV spectrometers, respectively. The IR spectra were recorded in KBr with a Bruker IFS 48 spectrophotometer. Melting points were measured with use of a Boethius apparatus and were uncorrected.

4.2. Syntheses

4.2.1. Compounds **2–10** (general procedure)

A reaction mixture containing **1** (0.1 g, 0.19 mmol), appropriate carboxylic acid (0.8 mmol), DIC (0.2 mL, 1.3 mmol), DMAP (0.05 g, 0.4 mmol), and DMF (20 mL) was protected from moisture and stirred at room temperature for 24 h. The crude product was

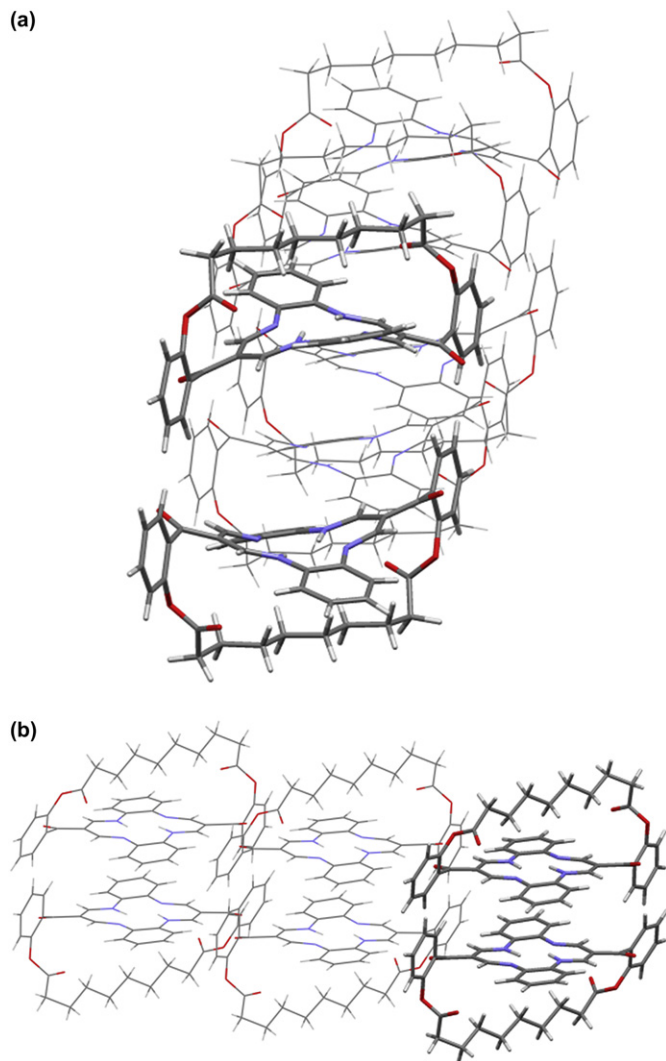


Figure 6. Dimers of **11** form a channel in **11a** (a) and a strand in **11b** (b).

Table 3
A conformation of tetraaza ring in **11a–c**

Molecule	Dihedral angle between planes of		
	Aliphatic chain/tetraaza ring [°]	<i>o</i> -Phenylene rings [°]	N–C–C–N fragments [°]
11a	0	31.47(12)	35.0(2)
11b	71.89(7)	6.6(2)	2.7(2)
11c (I)	74.90(10)	3.19(5)	1.23(3)
11c (II)	7.62(6)	9.27(6)	4.84(4)

precipitated by addition of water, filtered off, dried, and chromatographed on a column of silica gel using toluene/acetone (10:1) as eluent. The main orange fraction was collected and evaporated to dryness.

4.2.1.1. 7,16-Bis[2-(octanoyloxy)benzoyl]-5,14-dihydrodibenzo[b,i]-[1,4,8,11]tetraazacyclotetradecine (2). Orange powder, yield 0.03 g (20%), mp 196 °C. Crystals suitable for X-ray measurements were grown from the mixture DMF/diethyl ether. ¹H NMR (500 MHz, CDCl₃, δ ppm): 0.77 (t, *J*=7.0 Hz, 6H, H^g), 1.0–1.4 (m, 16H, H^{c–f}), 1.61 (m, *J*=7.0 Hz, 4H, H^b), 2.45 (t, *J*=7.0 Hz, 4H, H^a), 7.12 (dd, *J*=3.5, 6.5 Hz, 4H, H^{1,4,10,13}), 7.18 (dd, *J*=1.5, 8.0 Hz, 2H, H²²), 7.23 (dd, *J*=3.5, 6.5 Hz, 4H, H^{2,3,11,12}), 7.33 (ddd, *J*=1.5, 8.0, 8.0 Hz, 2H, H²³), 7.44 (dd, *J*=1.5, 8.0 Hz, 2H, H²⁵), 7.51 (ddd, *J*=1.5, 8.0, 8.0 Hz, 2H, H²⁴), 8.56 (d, *J*=6.0 Hz, 4H, H^{6,8,15,17}), 14.38 (t, *J*=6.5 Hz, 2H, H–N^{5,14}); ¹³C NMR

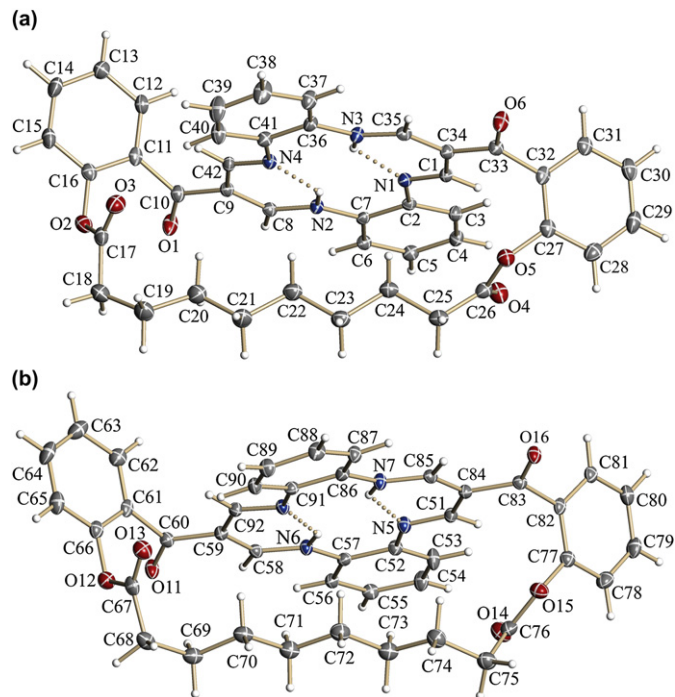


Figure 7. An ORTEP view of **11c** at 85 K with numbering scheme (molecules I and II). Displacement ellipsoids are drawn at the 50% probability level. Hydrogen atoms are drawn with an arbitrary radius.

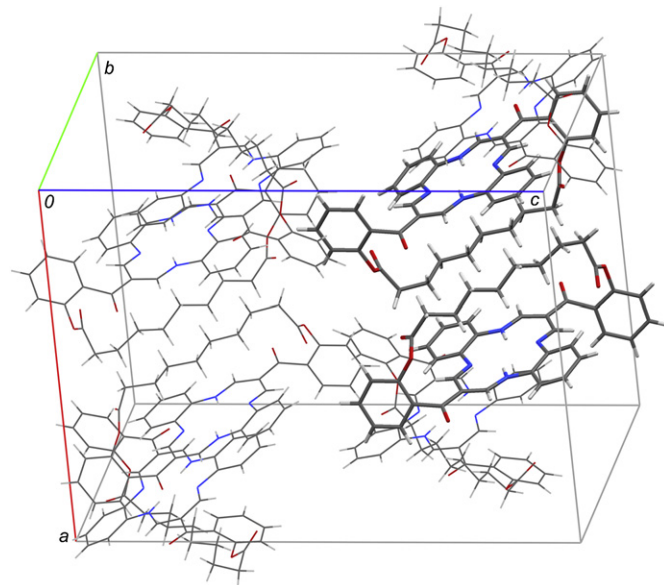


Figure 8. Packing diagram of the unit cell of compound **11c**.

(125 MHz, CDCl₃, δ ppm): 13.9 (C^g), 22.51 (C^f), 28.9+28.99 (C^{c,d}), 31.6 (C^b), 34.2 (C^a), 110.1 (C²⁰), 115.7 (C^{1,4,10,13}), 123.3, 126.0, 126.7, 129.0, 130.9, 133.0, 136.9, 147.7, 152.9 (C^{6,8,15,17}), 172.3 (C²⁶), 191.4 (C¹⁹); IR (KBr) ν_{max} (cm^{−1}): 3482, 3073, 2953, 2925, 2854, 1756, 1651, 1616; ESI-MS (*m/z*): 781.5 (M+H)⁺. Anal. Calcd for C₄₈H₅₂N₄O₆: C, 73.82; H, 6.71; N, 7.17. Found: C, 73.94; H, 6.74; N, 7.18%.

4.2.1.2. 7,16-Bis[2-(decanoyloxy)benzoyl]-5,14-dihydrodibenzo[b,i]-[1,4,8,11]tetraazacyclotetradecine (3). Orange powder, yield 0.030 g (19%), mp 174 °C. ¹H NMR (500 MHz, CDCl₃, δ ppm): 0.82 (t, *J*=7.0 Hz, 6H, H^g), 1.1–1.4 (m, 24H, H^{c–h}), 1.61 (m, *J*=7.0 Hz, 4H, H^b)

Table 4
Hydrogen bond geometry [Å and °]

D–H...A	D–H	H...A	D...A	D–H...A
2				
N(1)–H(1)...N(2) ^{1-x,1-y,1-z}	0.88(2)	2.06(2)	2.7442(14)	134.6(13)
11a				
N(2)–H(2N)...N(1) ^{1-x,y,3/2-z}	0.82(10)	2.04(10)	2.697(7)	138(8)
11b				
N(1)–H(1N)...N(3)	0.88	2.06	2.743(3)	133
N(4)–H(4N)...N(2)	0.88	2.07	2.747(3)	132
11c				
N(2)–H(2N)...N(4)	0.87(2)	2.06(1)	2.7557(15)	136.7(13)
N(3)–H(3N)...N(1)	0.85(2)	2.10(1)	2.7618(14)	134.0(13)
N(6)–H(6N)...N(8)	0.88(2)	2.08(2)	2.7612(15)	134.4(14)
N(7)–H(7N)...N(5)	0.86(2)	2.10(2)	2.7717(15)	134.8(14)

2.45 (t, $J=7.0$ Hz, 4H, H^a), 7.11 (dd, $J=3.5$, 6.5 Hz, 4H, H^{1,4,10,13}), 7.18 (dd, $J=1.5$, 8.0 Hz, 2H, H²²), 7.23 (dd, $J=3.5$, 6.5 Hz, 4H, H^{2,3,11,12}), 7.33 (ddd, $J=1.5$, 8.0, 8.0 Hz, 2H, H²³), 7.44 (dd, $J=1.5$, 8.0 Hz, 2H, H²⁵), 7.51 (ddd, $J=1.5$, 8.0, 8.0 Hz, 2H, H²⁴), 8.55 (d, $J=6.8$ Hz, 4H, H^{6,8,15,17}), 14.38 (t, $J=6.5$ Hz, 2H, H–N^{5,14}); ¹³C NMR (125 MHz, CDCl₃, δ ppm): 14.1 (Cⁱ), 22.6 (C^h), 24.8 (C^g), 29.0 (C^c), 29.2 (C^{d,f}), 29.3 (C^e), 31.8 (C^b), 34.2 (C^a), 110.0 (C²⁰), 115.7 (C^{1,4,10,13}), 123.3, 126.0, 126.8, 129.0, 130.9, 133.0, 136.9, 147.7, 152.9 (C^{6,8,15,17}), 172.3 (C²⁶), 191.3 (C¹⁹); IR (KBr) ν_{\max} (cm^{−1}): 3482, 3073, 2953, 2925, 2854, 1756, 1651, 1616; ESI-MS (m/z): 837.5 (M+H)⁺. Anal. Calcd for C₅₂H₆₀N₄O₆: C, 74.61; H, 7.22; N, 6.69. Found: C, 74.54; H, 7.06; N, 6.87%.

4.2.1.3. 7,16-Bis[2-(dodecanoyloxy)benzoyl]-5,14-dihydrodibenzo[b,i]-[1,4,8,11]tetraazacyclotetradecine (4). Orange powder, yield 0.059 g (35%), mp 141 °C. ¹H NMR (500 MHz, CDCl₃, δ ppm): 0.86 (t, $J=7.0$ Hz, 6H, H^k), 1.1–1.4 (m, 32H, H^{c–j}), 1.61 (m, $J=7.0$ Hz, 4H, H^b), 2.45 (t, $J=7.0$ Hz, 4H, H^a), 7.12 (dd, $J=3.5$, 6.5 Hz, 4H, H^{1,4,10,13}), 7.18 (dd, $J=1.5$, 8.0 Hz, 2H, H²²), 7.23 (dd, $J=3.5$, 6.5 Hz, 4H, H^{2,3,11,12}), 7.33 (ddd, $J=1.5$, 8.0, 8.0 Hz, 2H, H²³), 7.45 (dd, $J=1.5$, 8.0 Hz, 2H, H²⁵), 7.51 (ddd, $J=1.5$, 8.0, 8.0 Hz, 2H, H²⁴), 8.56 (d, $J=6.3$ Hz, 4H, H^{6,8,15,17}), 14.38 (t, $J=6.5$ Hz, 2H, H–N^{5,14}); ¹³C NMR (125 MHz, CDCl₃, δ ppm): 14.1 (C^k), 22.6 (C^j), 24.8 (C^b), 29.0 (C^c), 29.2 (C^d), 29.3 (C^h), 29.4 (C^e), 29.5 (C^{f,g}), 31.9 (Cⁱ), 34.2 (C^a), 110.7 (C²⁰), 115.8 (C^{1,4,10,13}), 123.3, 126.0, 126.8, 129.0, 130.9, 133.0, 136.9, 147.7, 152.9 (C^{6,8,15,17}), 172.3 (C²⁶), 191.3 (C¹⁹); IR (KBr) ν_{\max} (cm^{−1}): 3448, 3070, 2953, 2924, 2852, 1767, 1651, 1619; ESI-MS (m/z): 893.5 (M+H)⁺. Anal. Calcd for C₅₆H₆₈N₄O₆: C, 75.31; H, 7.67; N, 6.27. Found: C, 75.35; H, 7.60; N, 6.50%.

4.2.1.4. 7,16-Bis[2-(pentadecanoyloxy)benzoyl]-5,14-dihydrodibenzo[b,i]-[1,4,8,11]tetraazacyclotetradecine (5). Orange powder, yield 0.159 g (86%), mp 110 °C. ¹H NMR (500 MHz, CDCl₃, δ ppm): 0.88 (t, $J=7.0$ Hz, 6H, Hⁿ), 1.1–1.4 (m, 44H, H^{c–m}), 1.61 (m, $J=7.0$ Hz, 4H, H^b), 2.45 (t, $J=7.0$ Hz, 4H, H^a), 7.11 (dd, $J=3.5$, 6.5 Hz, 4H, H^{1,4,10,13}), 7.18 (dd, $J=1.5$, 8.0 Hz, 2H, H²²), 7.22 (dd, $J=3.5$, 6.5 Hz, 4H, H^{2,3,11,12}), 7.33 (ddd, $J=1.5$, 8.0, 8.0 Hz, 2H, H²³), 7.45 (dd, $J=1.5$, 8.0 Hz, 2H, H²⁵), 7.51 (ddd, $J=1.5$, 8.0, 8.0 Hz, 2H, H²⁴), 8.56 (d, $J=6.1$ Hz, 4H, H^{6,8,15,17}), 14.38 (t, $J=6.5$ Hz, 2H, H–N^{5,14}); ¹³C NMR (125 MHz, CDCl₃, δ ppm): 14.0 (Cⁿ), 22.6 (C^m), 24.7 (C^b), 29.0 (C^c), 29.2 (C^d), 29.3 (C^k), 29.6 (C^{f–j}), 31.9 (C^l), 34.2 (C^a), 110.0 (C²⁰), 115.7 (C^{1,4,10,13}), 123.3, 125.9, 126.7, 129.0, 130.8, 133.0, 136.9, 147.7, 152.8 (C^{6,8,15,17}), 172.2 (C²⁶), 191.3 (C¹⁹); IR (KBr) ν_{\max} (cm^{−1}): 3475, 3066, 2921, 2850, 1747, 1650, 1605; ESI-MS (m/z): 977.7 (M+H)⁺. Anal. Calcd for C₆₂H₈₀N₄O₆: C, 76.19; H, 8.25; N, 5.73. Found: C, 76.06; H, 8.21; N, 5.56%.

4.2.1.5. 7,16-Bis[2-(hexadecanoyloxy)benzoyl]-5,14-dihydrodibenzo[b,i]-[1,4,8,11]tetraazacyclotetradecine (6). Orange powder, yield 0.14 g (73%), mp 119 °C. ¹H NMR (500 MHz, CDCl₃, δ ppm): 0.88 (t, $J=7.0$ Hz, 6H, H^o), 1.1–1.4 (m, 48H, H^{c–n}), 1.61 (m, $J=7.0$ Hz, 4H, H^b),

2.45 (t, $J=7.0$ Hz, 4H, H^a), 7.11 (dd, $J=3.5$, 6.5 Hz, 4H, H^{1,4,10,13}), 7.18 (dd, $J=1.5$, 8.0 Hz, 2H, H²²), 7.22 (dd, $J=3.5$, 6.5 Hz, 4H, H^{2,3,11,12}), 7.33 (ddd, $J=1.5$, 8.0, 8.0 Hz, 2H, H²³), 7.45 (dd, $J=1.5$, 8.0 Hz, 2H, H²⁵), 7.51 (ddd, $J=1.5$, 8.0, 8.0 Hz, 2H, H²⁴), 8.56 (d, $J=6.2$ Hz, 4H, H^{6,8,15,17}), 14.37 (t, $J=6.5$ Hz, 2H, H–N^{5,14}); ¹³C NMR (125 MHz, CDCl₃, δ ppm): 14.1 (C^o), 22.7 (Cⁿ), 24.8 (C^b), 29.0 (C^c), 29.2 (C^d), 29.3 (C^l), 29.6 (C^{f–k}), 31.9 (C^m), 34.2 (C^a), 110.1 (C²⁰), 115.7 (C^{1,4,10,13}), 123.3, 125.9, 126.8, 129.0, 130.9, 133.0, 137.0, 147.7, 152.9 (C^{6,8,15,17}), 172.3 (C²⁶), 191.3 (C¹⁹); IR (KBr) ν_{\max} (cm^{−1}): 3462, 3064, 2990, 2920, 2849, 1744, 1650, 1603; ESI-MS (m/z): 1005.7 (M+H)⁺. Anal. Calcd for C₆₄H₈₄N₄O₆: C, 76.46; H, 8.42; N, 5.57. Found: C, 76.24; H, 8.31; N, 5.33%.

4.2.1.6. 7,16-Bis[2-(6-phenylhexanoyloxy)benzoyl]-5,14-dihydrodibenzo[b,i]-[1,4,8,11]tetraazacyclotetradecine (7). Orange powder, yield 0.106 g (64%), mp 163 °C. ¹H NMR (500 MHz, CDCl₃, δ ppm): 1.31 (m, 4H, H^c), 1.52 (m, 4H, H^d), 1.64 (m, 4H, H^b), 2.46 (m, 8H, H^{a,e}), 7.03–7.21 (m, 20H, H^{f,g,i,1–4,10–13,22}), 7.32 (ddd, $J=1.5$, 7.5, 7.5 Hz, 2H, H²³), 7.43 (dd, $J=1.5$, 7.5 Hz, 2H, H²⁵), 7.50 (ddd, $J=1.5$, 7.5, 7.5 Hz, 2H, H²⁴), 8.54 (d, $J=6.3$ Hz, 4H, H^{6,8,15,17}), 14.38 (t, $J=6.5$ Hz, 2H, H–N^{5,14}); ¹³C NMR (125 MHz, CDCl₃, δ ppm): 24.5 (C^b), 28.5 (C^c), 30.8 (C^d), 34.0 (C^a), 35.5 (C^e), 110.0 (C²⁰), 115.7 (C^{1,4,10,13}), 123.2, 123.5 (Cⁱ), 125.9, 126.7, 128.1+128.2 (C^{g,i}), 129.0, 130.9, 132.9, 136.9, 142.3 (C^f), 147.6, 152.8 (C^{6,8,15,17}), 172.1 (C²⁶), 191.3 (C¹⁹); IR (KBr) ν_{\max} (cm^{−1}): 3445, 3061, 2926, 2853, 1758, 1650, 1619; ESI-MS (m/z): 877.5 (M+H)⁺. Anal. Calcd for C₅₆H₅₂N₄O₆: C, 76.69; H, 5.98; N, 6.39. Found: C, 76.46; H, 6.03; N, 6.33%.

4.2.1.7. 7,16-Bis[2-(11-phenoxyundecanoyloxy)benzoyl]-5,14-dihydrodibenzo[b,i]-[1,4,8,11]tetraazacyclotetradecine (8). Orange powder, yield 0.129 g (66%), mp 102 °C. ¹H NMR (500 MHz, CDCl₃, δ ppm): 1.15–1.4 (m, 24H, H^{c–g}), 1.45 (m, 4H, H^h), 1.61 (m, 4H, H^b), 1.71 (m, 4H, Hⁱ), 2.45 (t, $J=7.5$ Hz, 4H, H^a), 3.9 (t, $J=6.5$ Hz, 4H, H^j), 6.86–6.94 (m, 8H, H^{l,m}), 7.10 (dd, $J=3.5$, 6.0 Hz, 4H, H^{1,4,10,13}), 7.18 (dd, $J=0.5$, 8.0 Hz, 2H, H²²), 7.21 (dd, $J=3.5$, 6.0 Hz, 4H, H^{2,3,11,12}), 7.30–7.36 (m, 4H, H^{n,23}), 7.44 (dd, $J=1.5$, 8.0 Hz, 2H, H²⁵), 7.50 (ddd, $J=1.5$, 8.0, 8.0 Hz, 2H, H²⁴), 8.50 (d, $J=6.0$ Hz, 4H, H^{6,8,15,17}), 14.38 (t, $J=6.5$ Hz, 2H, H–N^{5,14}); ¹³C NMR (125 MHz, CDCl₃, δ ppm): 24.7 (C^b), 26.0 (C^d), 28.9–29.5 (C^{c–g}), 34.2 (C^a), 67.8 (C^j), 110.0 (C²⁰), 114.5 (C^l), 115.7 (C^{1,4,10,13}), 120.4 (Cⁿ), 123.3, 126.0, 126.8, 129.4 (C^m), 130.9, 133.0, 136.9, 147.7, 152.9 (C^{6,8,15,17}), 159.1 (C^k), 172.3 (C²⁶), 191.4 (C¹⁹); IR (KBr) ν_{\max} (cm^{−1}): 3476, 3061, 2931, 2918, 2849, 1747, 1656, 1611; ESI-MS (m/z): 1049.6 (M+H)⁺. Anal. Calcd for C₆₆H₇₂N₄O₆: C, 75.55; H, 6.92; N, 5.34. Found: C, 75.61; H, 6.82; N, 5.45%.

4.2.1.8. 7,16-Bis[2-(pivaloyloxy)benzoyl]-5,14-dihydrodibenzo[b,i]-[1,4,8,11]tetraazacyclotetradecine (9). Orange powder, yield 0.04 g (30%), mp 270 °C. ¹H NMR (500 MHz, CDCl₃, δ ppm): 1.21 (s, 18H, H^b), 7.12 (dd, $J=3.5$, 6.5 Hz, 4H, H^{1,4,10,13}), 7.15 (dd, $J=0.5$, 6.0 Hz, 4H, H²²), 7.23 (dd, $J=3.5$, 6.5 Hz, 4H, H^{2,3,11,12}), 7.34 (ddd, $J=1.5$, 8.0, 8.0 Hz, 2H, H²³), 7.45 (dd, $J=1.5$, 8.0 Hz, 2H, H²⁵), 7.50 (ddd, $J=1.5$, 8.0, 8.0 Hz, 2H, H²⁴), 8.54 (br s, 4H, H^{6,8,15,17}), 14.34 (t, $J=6.5$ Hz, 2H, H–N^{5,14}); ¹³C NMR (125 MHz, CDCl₃, δ ppm): 26.4 (C^b), 39.0 (C^a), 110.3 (C²⁰), 115.8 (C^{1,4,10,13}), 123.1, 126.0, 126.8, 129.0, 130.9, 133.0, 137.0, 147.8, 152.9 (C^{6,8,15,17}), 176.9 (C²⁶), 191.3 (C¹⁹); IR (KBr) ν_{\max} (cm^{−1}): 3471, 3066, 2976, 2933, 2872, 1747, 1648, 1616; ESI-MS (m/z): 697.5 (M+H)⁺. Anal. Calcd for C₄₂H₄₀N₄O₆: C, 72.40; H, 5.79; N, 8.04. Found: C, 72.34; H, 5.71; N, 8.29%.

4.2.1.9. 7,16-Bis[2-(2-naphthylacyloxy)benzoyl]-5,14-dihydrodibenzo[b,i]-[1,4,8,11]tetraazacyclotetradecine (10). Orange powder, yield 0.03 g (18%), mp 170 °C. ¹H NMR (500 MHz, CDCl₃, δ ppm): 3.90 (s, 4H, H^a), 7.05 (dd, $J=3.5$, 6.0 Hz, 4H, H^{1,4,10,13}), 7.09 (dd, $J=3.5$, 6.5 Hz, 4H, H^{2,3,11,12}), 7.13 (m, 4H, H^{e,f}), 7.22 (dd, $J=0.5$, 8.0 Hz, 2H, H²²), 7.29 (dd, $J=2.0$, 8.5 Hz, 2H, H²⁵), 7.35 (ddd, $J=1.0$, 7.5, 7.5 Hz, 2H, H²³), 7.40–7.46 (m, 6H, H^{g–i}), 7.5 (m, 4H, H^{d,24}), 7.61 (s, 2H, H^c), 8.26 (d,

$J=4.7$ Hz, 4H, $H^{6,8,15,17}$), 13.54 (t, $J=6.5$ Hz, 2H, $H-N^{5,14}$); ^{13}C NMR (125 MHz, $CDCl_3$, δ ppm): 41.5 (C^a), 109.8 (C^{20}), 115.5 ($C^{1,4,10,13}$), 123.1, 125.6, 126.0, 126.4, 126.5, 127.0, 127.3, 127.4, 128.0, 128.2, 129.1, 130.8, 132.4, 133.1, 133.3, 136.6, 147.2, 152.0 ($C^{6,8,15,17}$), 169.9 (C^{26}), 190.9 (C^{19}); IR (KBr) ν_{max} (cm^{-1}): 3434, 3056, 2969, 2928, 2874, 1700, 1654, 1599; ESI-MS (m/z): 865.6 ($M+H$)⁺. Anal. Calcd for $C_{56}H_{40}N_4O_6$: C, 77.76; H, 4.66; N, 6.48. Found: C, 77.53; H, 4.71; N, 6.28%.

4.2.2. Compounds **11**–**13** (general procedure)

A reaction mixture containing **1** (0.1 g, 0.19 mmol), appropriate dicarboxylic acid (0.3 mmol), DIC (0.2 mL, 1.3 mmol), DMAP (0.05 g, 0.4 mmol), and DMF (20 mL) was protected from moisture and stirred at room temperature for 48 h. Dichloromethane was added (50 mL) and the whole mixture transferred to a separating funnel. It was washed thoroughly with water (5×100 mL) and then dried over anhydrous magnesium sulfate. The solvents were removed under reduced pressure on a rotary evaporator and the residue was chromatographed on a column of silica gel. The main orange fraction was collected and evaporated to dryness.

4.2.2.1. Lacunar compound 11. Eluent: toluene/ethyl acetate (1:1). Orange powder, yield 0.076 g (58%), mp $>260^\circ C$. Crystals suitable for X-ray measurements were grown from chloroform (**11a**); by slow diffusion of water into the solution of **11** in DMF (**11b**) and from the mixture of DMF/diisopropyl ether (**11c**). 1H NMR (500 MHz, $CDCl_3$, δ ppm): 0.95–1.15 (m, 8H, $H^{c,d}$), 1.46 (qu, $J=7.5$ Hz, 4H, H^b), 2.41 (t, $J=7.3$ Hz, 4H, H^a), 7.12 (dd, $J=3.4$, 6.2 Hz, 4H, $H^{2,3,11,12}$), 7.19 (dd, $J=1.1$, 8.4 Hz, 2H, H^{22}), 7.24 (dd, $J=3.5$, 6.1 Hz, 4H, $H^{1,4,10,13}$), 7.38 (ddd, $J=1.2$, 7.5, 7.5 Hz, 2H, H^{24}), 7.52 (d, $J=7.4$ Hz, 2H, H^{25}), 7.54 (ddd, $J=1.7$, 7.5, 7.5 Hz, 2H, H^{23}), 8.53 (d, $J=6.3$ Hz, 4H, $H^{6,8,15,17}$), 14.34 (t, $J=6.7$ Hz, 2H, $H-N^{5,14}$); ^{13}C NMR (75 MHz, $CDCl_3$, δ ppm): 24.8 (C^b), 29.1, 29.2 ($C^{c,d}$), 34.3 (C^a), 110.5 (C^{20}), 115.3 ($C^{1,4,10,13}$), 123.1 (C^{22}), 126.5 (C^{24}), 126.7 ($C^{2,3,11,12}$), 129.3 (C^{25}), 131.0 (C^{23}), 132.9 ($C^{7,16}$), 136.4 ($C^{5a,9a,14a,18a}$), 147.2 (C^{21}), 152.1 ($C^{6,8,15,17}$), 172.2 (C^{26}), 191.5 (C^{19}); IR (KBr) ν_{max} (cm^{-1}): 3066, 2932, 2854, 1749; ESI-MS (m/z): 695.3 ($M+1$)⁺. Anal. Calcd for $C_{42}H_{38}N_4O_6$: C, 72.61; H, 5.51; N, 8.06. Found: C, 72.78; H, 5.30; N, 7.96%.

4.2.2.2. Lacunar compound 12. Eluent: toluene/chloroform (5:1). Orange powder, yield 0.055 g (41%), mp $>280^\circ C$. 1H NMR (500 MHz, $CDCl_3$, δ ppm): 2.78 (m, 8H, $H^{a,b}$), 6.90 (s, 4H, H^d), 7.1–7.22 (m, 8H, $H^{1-4,10-13}$), 7.25 (dd, $J=7.5$, 7.5 Hz, 2H, H^{24}), 7.39 (ddd, $J=7.5$, 7.5, 1.0 Hz, 2H, H^{23}), 7.5–7.6 (m, 4H, $H^{22,25}$), 8.50 (d, $J=4.7$ Hz, 4H, $H^{6,8,15,16}$), 14.35 (t, $J=6.5$ Hz, 2H, $H-N^{5,14}$); ^{13}C NMR (125 MHz, $CDCl_3$, δ ppm): 29.7 (C^b), 35.4 (C^a), 110.5 (C^{20}), 115.4 ($C^{1,4,10,13}$), 123.2 (C^{22}), 126.2 (C^{24}), 126.8 ($C^{2,3,11,12}$), 128.1 (C^d), 129.6 (C^{25}), 131.2 (C^{23}), 132.8 ($C^{7,16}$), 136.4 ($C^{5a,9a,14a,18a}$), 137.6 (C^c), 147.5 (C^{21}), 152.3 ($C^{6,8,15,17}$), 171.3 (C^{26}), 191.1 (C^{19}); IR (KBr) ν_{max} (cm^{-1}): 3441, 3064, 3019, 2962, 2926, 2854, 1755, 1651, 1613, 1563; MALDI-MS (m/z): 714.21 (M^+). Anal. Calcd for $C_{44}H_{34}N_4O_6$: C, 73.94; H, 4.79; N, 7.84. Found: C, 74.02; H, 4.65; N, 7.91%.

4.2.2.3. Lacunar compound 13. Eluent: toluene/chloroform (5:1). Orange powder, yield 0.079 g (64%), mp $>280^\circ C$. 1H NMR (500 MHz, $CDCl_3$, δ ppm): 7.12 (s, 8H, $H^{1-4,10-13}$), 7.36 (d, $J=8.0$ Hz, 2H, H^{22}), 7.48 (dd, $J=7.5$, 7.5 Hz, 2H, H^{24}), 7.63 (ddd, $J=7.6$, 7.6, 1.6 Hz, 2H, H^{23}), 7.81 (dd, $J=1.6$, 7.6 Hz, 2H, H^{25}), 7.94 (s, 4H, H^b), 8.32 (d, $J=6.4$ Hz, 4H, $H^{6,8,15,17}$), 13.84 (t, $J=6.3$ Hz, 2H, $H-N^{5,14}$); ^{13}C NMR (125 MHz, $CDCl_3$, δ ppm): 110.9 (C^{20}), 115.8 ($C^{1,4,10,13}$), 122.4 (C^{22}), 126.7 ($C^{2,3,11,12}$), 126.9 (C^{24}), 129.9 (C^b), 131.1 (C^{25}), 132.1 ($C^{7,16}$), 133.1 (C^a), 136.7 ($C^{5a,9a,14a,18a}$), 147.7 (C^{21}), 152.0 ($C^{6,8,15,17}$), 163.2 (C^{26}), 190.5 (C^{19}); IR (KBr) ν_{max} (cm^{-1}): 3467, 3061, 3012, 2931, 2866, 1744, 1670, 1614, 1564; MALDI-MS (m/z): 658.34 (M^+). Anal. Calcd for $C_{40}H_{26}N_4O_6 \cdot DMF$: C, 70.58; H, 4.55; N, 9.57. Found: C, 70.63; H, 4.61; N, 9.52%.

5. Crystallography

Structures of compounds **2** and **11a–11c** were determined by single-crystal X-ray diffraction technique. Intensity data for the crystals of **2**, **11a**, and **11c** were collected using a Bruker AXS Smart APEX-II CCD 3-circle diffractometer with MonoCap capillary and graphite-monochromated Mo $K\alpha$ radiation ($\lambda=0.71073$ Å, 50 kV, 32 mA) at 100, 85, and 90 K, respectively; 2700 frames were measured at 0.4° ω -scans with a counting time of 12, 5, and 10 s/frame, respectively. Data collection and data reduction were done with the SMART and SAINT-PLUS programs.^{18,19}

Measurements for **11b** were performed on a Kuma KM4CCD κ -axis diffractometer with graphite-monochromated Mo $K\alpha$ radiation ($\lambda=0.71073$ Å, 50 kV, 40 mA) at 200 K; 1204 frames were measured at 1.0° intervals with a counting time of 30 s/frame. Data collection and data reduction were carried out with the Oxford Diffraction programs.²⁰ The structures were solved by direct methods by using the SHELXS-97 program.²¹ All non-hydrogen atoms were refined anisotropically by full-matrix least-squares based on F^2 using the SHELXL-97 program.²¹ The final geometrical calculations were carried out with the PLATON program.²² The relevant crystal data and experimental details are summarized in Table 1.

Hydrogen atoms were placed in calculated positions, and refined using a riding model (for **11b** and **11c**) or refined freely (for **2** and **11a**). Figures were drawn using Mercury and SHELXTL programs.^{23,19}

6. Crystallographic data

Crystallographic data for the structures reported in this paper have been deposited with the Cambridge Crystallographic Data Center as supplementary publication nos. CCDC 677274 (compound **2**), CCDC 677275 (compound **11a**), CCDC 677276 (compound **11b**), and CCDC 677277 (compound **11c**). Copies of the data can be obtained free of charge on application to CCDC, 12 Union Road, Cambridge CB2 1EZ, UK (fax: +44 1223 336 033; e-mail: deposit@ccdc.cam.ac.uk).

References and notes

- Mountford, P. *Chem. Soc. Rev.* **1998**, 27, 105–115 and references therein.
- (a) Weiss, M. C.; Gordon, G.; Goedken, V. L. *Inorg. Chem.* **1977**, 16, 305–310; (b) Azuma, N.; Tani, H.; Ozawa, T.; Niida, H.; Tajima, K. *J. Chem. Soc., Perkin Trans. 2* **1995**, 343–348; (c) Rihs, G.; Sigg, I.; Haas, G.; Winkler, T. *Helv. Chim. Acta* **1985**, 68, 1933–1935; (d) Grolík, J.; Sieroń, L.; Eilmes, J. *Tetrahedron Lett.* **2006**, 47, 8209–8213.
- (a) Goedken, V. L.; Pluth, J. J.; Peng, S. M.; Bursten, B. J. *Am. Chem. Soc.* **1976**, 98, 8014–8021; (b) Cotton, F. A.; Czuchajowska, J. *Polyhedron* **1990**, 9, 2553–2566 and references therein; (c) Desiraju, G. R. *Acc. Chem. Res.* **1996**, 29, 441–449; (d) Desiraju, G. R.; Kashino, S.; Coombs, M. M.; Glusker, J. P. *Acta Crystallogr.* **1993**, B49, 880–892.
- (a) Andrews, P. C.; Atwood, J. L.; Barbour, L. J.; Nichols, P. J.; Raston, C. J. *Chem.—Eur. J.* **1998**, 4, 1384–1387; (b) Andrews, P. C.; Hardie, M. J.; Nichols, P. J.; Raston, C. L. *Coord. Chem. Rev.* **1999**, 189, 169–198; (c) Hardie, M. J.; Nichols, P. J.; Raston, C. L. *Advanced Supramolecular Chemistry*; Gokel, G. W., Ed.; Cerberus: 2002; Vol. 8, pp 26–36.
- (a) Andrews, P. C.; Atwood, J. L.; Barbour, L. J.; Croucher, P. D.; Nichols, P. J.; Smith, N. O.; Skelton, B. W.; White, A. H.; Raston, C. L. *J. Chem. Soc., Dalton Trans.* **1999**, 2927–2932; (b) Eilmes, J.; Ptaszek, M.; Woźniak, K. *Polyhedron* **2002**, 21, 7–17; (c) Lewiński, K.; Eilmes, J. *J. Incl. Phenom. Macrocycl. Chem.* **2005**, 52, 261–266.
- (a) Pawlica, D.; Radic Stojkovic, M.; Sieroń, L.; Piantanida, I.; Eilmes, J. *Tetrahedron* **2006**, 62, 9156–9165; (b) Radić-Stojković, M.; Piantanida, I.; Kralj, M.; Marjanović, M.; Žinić, M.; Pawlica, D.; Eilmes, J. *Bioorg. Med. Chem.* **2007**, 15, 1795–1801.
- Buckley, B. R. In *Comprehensive Organic Functional Group Transformations II*; Katritzky, A. R., Taylor, R. J. K., Eds.; Elsevier: Oxford, 2005; Vol. 5, Chapter 5.03, p 131.
- Bailey, P. D.; Mills, T. J.; Pettecrew, R.; Price, R. A. In *Comprehensive Organic Functional Group Transformation II*; Katritzky, A. R., Taylor, R. J. K., Eds.; Elsevier: Oxford, 2005; Vol. 5, Chapter 5.06, p 223.
- (a) Chang, C. K. *J. Am. Chem. Soc.* **1977**, 99, 2821–2822; (b) Collman, J. P.; Brauman, J. I.; Fitzgerald, J. P.; Hampton, P. D.; Naruta, Y.; Sparapany, J. W.; Ibers, J. A. *J. Am. Chem. Soc.* **1988**, 110, 3477–3486; (c) Collman, J. P.; Zhang, X.

- Comprehensive Supramolecular Chemistry*; Atwood, J. L., Davies, J. E. D., MacNicol, D. D., Vögtle, F., Eds.; Pergamon: Oxford, New York, NY, 1996; Vol. 5, pp 1–32; and references therein; (d) Momenteau, M.; Reed, C. A. *Chem. Rev.* **1994**, *94*, 659–698 and references therein.
10. (a) Ransohoff, S.; Adams, M. T.; Dzuga, S. J.; Busch, D. H. *Inorg. Chem.* **1990**, *29*, 2945–2947; (b) Davis, W. M.; Dzuga, S. J.; Glogowski, M. W.; Delgado, R.; Busch, D. H. *Inorg. Chem.* **1991**, *30*, 2724–2731; (c) Ramprasad, D.; Lin, W. K.; Goldsby, K. A.; Busch, D. H. *J. Am. Chem. Soc.* **1988**, *110*, 1480–1487; (d) Busch, D. H.; Alcock, N. W. *Chem. Rev.* **1994**, *94*, 585–623 and references therein.
11. Hardie, M. J.; Malic, N.; Nichols, P. J.; Raston, C. L. *Tetrahedron Lett.* **2001**, *42*, 8075–8079.
12. (a) Alcock, N. W.; Lin, W. K.; Jircitano, A.; Mokren, J. D.; Corfield, P. W. R.; Johnson, G.; Novotnak, G.; Cairns, C.; Busch, D. H. *Inorg. Chem.* **1987**, *26*, 440–452; (b) Busch, D. H. *Chem. Rev.* **1993**, *93*, 847–860 and references therein; (c) Sakata, K.; Saitoh, Y.; Kawakami, K.; Nakamura, N.; Hori, T.; Nakano, Y.; Hashimoto, M. *Synth. React. Met.-Org. Chem.* **1996**, *26*, 1267–1278 and references therein.
13. (a) Malone, J. F.; Murray, C. M.; Charlton, M. H.; Docherty, R.; Lavery, A. J. *J. Chem. Soc., Faraday Trans.* **1997**, *93*, 3429–3436; (b) Desiraju, G. R.; Steiner, T. *The Weak Hydrogen Bond in Structural Chemistry and Biology*; Oxford University Press: New York, NY, 1999; (c) Ciunik, Z.; Desiraju, G. R. *Chem. Commun.* **2001**, 703–704.
14. Meyer, E. A.; Castellano, R. K.; Diederich, F. *Angew. Chem., Int. Ed.* **2003**, *42*, 1210–1250.
15. Bond, A. D. *Chem. Commun.* **2002**, 1664–1665.
16. (a) Kuzmich, R.; Dobrzycki, L.; Wozniak, K.; Benevelli, F.; Klinowski, J.; Kolodziejewski, W. *Phys. Chem. Chem. Phys.* **2002**, *4*, 2387–2391; (b) Pietraszkiewicz, M.; Pietraszkiewicz, O.; Kolodziejewski, W.; Wozniak, K.; Feeder, N.; Benevelli, F.; Klinowski, J. *J. Phys. Chem. B* **2000**, *104*, 1921–1926.
17. Sigg, I.; Haas, G.; Winkler, T. *Helv. Chim. Acta* **1982**, *65*, 275–279.
18. Bruker. *SMART for WNT/2000. Version 5.630*; Bruker AXS: Madison, Wisconsin, USA, 2002.
19. Bruker. *SAINT-Plus (Version 6.45) and SHELXTL (Version 6.14)*; Bruker AXS: Madison, Wisconsin, USA, 2003.
20. Oxford Diffraction. *CrysAlis CCD and CrysAlis RED. Version 1.171*; Oxford Diffraction: Abingdon, Oxfordshire, England, 2006.
21. Sheldrick, G. M. *Acta Crystallogr.* **2008**, *A64*, 112–122.
22. Spek, A. L. *J. Appl. Crystallogr.* **2003**, *36*, 7–13.
23. Macrae, C. F.; Edgington, P. R.; McCabe, P.; Pidcock, E.; Shields, G. P.; Taylor, R.; Towler, M.; van de Streek, J. *J. Appl. Crystallogr.* **2006**, *39*, 453–457.